The American Journal of Pathology, Vol. 174, No. 4, April 2009

DOI: 10.2353/ajpath.2009.080654

Cardiovascular, Pulmonary and Renal Pathology

Alterations in Fatty Acid Utilization and an Impaired Antioxidant Defense Mechanism Are Early Events in Podocyte Injury

A Proteomic Analysis

Corina Mayrhofer,*† Sigurd Krieger,* Nicole Huttary,* Martina Wei-Fen Chang,‡ Johannes Grillari,‡§ Günter Allmaier,† and Dontscho Kerjaschki*

From the Clinical Institute of Pathology, Medical University of Vienna, Vienna; the Institute of Chemical Technologies and Analytics,† Vienna University of Technology, Vienna; the Institute of Applied Microbiology,‡ University of Natural Resources and Applied Life Sciences, Vienna; and BMT Research Vienna,§ Vienna, Austria*

Ultrastructural alterations of podocytes are closely associated with loss of glomerular filtration function. In the present study, we explored changes at the proteome level that paralleled the disturbances of podocyte architecture in the early stages of puromycin aminonucleoside (PA) nephrosis *in vivo*. Using two-dimensional fluorescence difference gel electrophoresis and vacuum matrix-assisted laser desorption/ionization mass spectrometry combined with postsource decay fragment ion analysis and high-energy collision-induced dissociation tandem mass spectrometry, 23 differentially expressed protein spots, corresponding to 16 glomerular proteins that are involved in various cellular functions, were unambiguously identified, and a subset was corroborated by Western blot analysis. The majority of these proteins were primarily related to fatty acid metabolism and redox regulation. Key enzymes of the mitochondrial β-oxidation pathway and antioxidant enzymes were consistently down-regulated in PA nephrosis. These changes were paralleled by increased expression levels of CD36. PA treatment of murine podocytes in culture resembled these specific protein changes *in vitro*. In this cell system, the modulatory effects of albumin-bound fatty acids on the expression levels of Mn-superoxide dismutase in response to PA were demonstrated as well. Taken together, these results indicate that a disrupted fatty acid metabolism in concert with an impaired antioxidant defense mechanism in podocytes may play a role in the early stages of PA-induced lesions in podocytes. *(Am J Pathol 2009, 174:1191–1202; DOI: 10.2353/ajpath.2009.080654)*

The renal glomerulus is the site of plasma ultrafiltration, allowing for the excretion of water and small molecules while retaining cells and essential plasma proteins.[1] The glomerular filtration barrier that is based on size,[2] shape,[3] and charge[2,4] selectivity is formed by fenestrated endothelial cells, the glomerular basement membrane, and visceral epithelial cells, known as podocytes. Alterations of this barrier correlate closely with an increase in glomerular permeability to proteins that cause proteinuria and eventually the nephrotic syndrome.[5,6] A morphological hallmark of many forms of renal proteinuric diseases, in general, is a change in podocyte architecture, including effacement and retraction of podocyte foot processes and dislocation of slit diaphragms.[7–10] In children, minimal change disease (MCD) is the most common form of nephrotic syndrome and in adults MCD accounts for 15 to 25% of nephrotic syndrome.[11] MCD is characterized by highly selective proteinuria, mainly albuminuria. Histopathological changes are restricted to podocyte foot

Supported by the Austrian Science Foundation (grant P15008 to G. A.) and the European Commission project (grant QLG1-CT2002-01215 to D.K.).

C.M. and S.K. contributed equally to this study.

Accepted for publication December 29, 2008.

Supplemental material for this article can be found on *http://ajp.amjpathol.org.*

Current address of C.M.: Institute of Cell and Molecular Biology, Division of Molecular Biometry, Uppsala University, Uppsala, Sweden.

Address reprint requests to Corina Mayrhofer, Clinical Institute of Pathology, Medical University of Vienna, Waehringer Gürtel 18-20, A-1090 Vienna, Austria. E-mail: corina.mayrhofer@meduniwien.ac.at.

processes that become extensively flattened and are not associated with glomerular inflammatory cell infiltrations. To study the molecular mechanisms underlying the ultrastructural alterations of podocytes, the injection of puromycin aminonucleoside (PA) in rats induces severe podocyte damage that closely resembles the human idiopathic MCD, both morphologically and functionally.[12,13] In this experimental disease several molecules were identified that play essential roles in the stability of the functional glomerular filtration barrier. These include podocyte-specific membrane proteins[14] as well as cytoskeletal proteins or cytoskeleton linking molecules.[15–17] Furthermore, reactive oxygen species (ROS) play a critical role in podocyte foot process effacement and glomerular dysfunction,[18–20] and enhanced lipid peroxidation (LPO) was reported in puromycin aminonucleoside nephrosis (PAN) as well as with other experimental and human glomerular diseases.[7,21–23] Recently, conditionally immortalized mouse podocytes[24] were used to investigate the effect of PA *in vitro*.[25,26] However, precise information on the intracellular molecular events that link the disturbances of podocyte architecture and increased glomerular permeability with any of these effector mechanisms is still incomplete.

Currently, the global study of proteins, their expression and/or their localization in normal as well as in pathological conditions is widely used to provide more information of pathogenic mechanisms.[27,28] Previous proteomic studies have been conducted to analyze changes in the glomerular proteome in a diabetic animal model[29] or in sclerosis.[30] We already applied proteomic methods including two-dimensional gel electrophoresis (2-D GE) to investigate cell surface proteins on glomerular cells.[31,32] The purpose of the present study is to characterize changes in protein expression accompanying early changes in PAN and thus to expand our understanding of the intracellular processes leading to podocyte injury related to proteinuria.

Materials and Methods

Primary Antibodies

Rabbit polyclonal IgG specific for superoxide dismutase 2 (Mn-SOD, used 1:5000) and rabbit polyclonal anti-peroxiredoxin-3 (PRDX3, used 1:10,000) IgG were obtained from Abcam (Cambridge, UK). Rabbit polyclonal anti-glyceraldehyde-3-phosphate dehydrogenase (GAPDH, used 1:3000) antibody was obtained from Trevigen (Gaithersburg, MD). Rabbit polyclonal anti-CD36 (used 1:300 unless otherwise stated) was obtained from Cayman Chemical (Ann Arbor, MI). Mouse monoclonal IgG specific for CD68 (used 1:200) was obtained from Serotec (Oxford, UK) and polyclonal IgY antibody specific for short-chain L-3-hydroxyacyl CoA dehydrogenase (HCDH, used 1:400) was obtained from Genway Biotech (San Diego, CA). Rabbit polyclonal specific for mitochondrial uncoupling protein 3 (UCP3, used 1:500) was purchased from Novus Biologicals (Littleton, CO) and mouse monoclonal specific for α-dystroglycan (α-DG, used 1:250) was obtained from Upstate Biotechnology (Lake Placid, NY).

Animals

Male Sprague-Dawley rats weighing 250 to 300 g were obtained from the Central Animal Laboratory of the Medical University of Vienna. The experimental use of animals was authorized by the Austrian Ministry of Science.

Induction of PAN

Rats fed with standard chow and free access to water were randomly divided into an experimental group (n = 6) and a control group (n = 6). PAN was induced by daily subcutaneous injection of 1.67 mg/100 g body weight of PA (P-7130; Sigma Aldrich, St. Louis, MO)[33,34] in Hanks' balanced salt solution (Gibco BRL, Paisley, UK) for 5 days. The control group received equal volume of Hanks' balanced salt solution. Rats were sacrificed under anesthesia 2 days after the last injection.

Histological Confirmation of Glomerular Alterations

Part of the kidney cortex was fixed in 4% paraformaldehyde in 0.1 mol/L phosphate buffer. After washing and postfixing in 1% OsO_4 the material was dehydrated and embedded in Epon resin. Ultrathin sections were prepared and stained with uranylacetate and lead citrate. Sections were examined under a JEM 1010 electron microscope (JEOL, Tokyo, Japan).

Two-Dimensional Fluorescence Difference Gel Electrophoresis (2-D DIGE) of Glomerular Proteins

Kidneys from animals in the control group and in the PAN group were perfused with Hanks' balanced salt solution and glomeruli were obtained by graded sieving of minced kidney cortex suspensions on ice as described previously[35] with minor modifications. Briefly, small pieces of minced kidney cortex were flushed through a 100-μm nylon strainer (BD Falcon, San Jose, CA) and the flow-through was further filtered through a 70-μm strainer. The purified glomeruli were then collected on the 70-μm strainer. The preparation consisted of >95% glomeruli when examined by phase-contrast microscopy. Glomeruli isolated from both kidneys of one individual animal were mixed and used as one sample of glomerular proteins. The sample complexity of the glomerular proteome was reduced by Triton X-114 phase separation.[36] Hydrophilic proteins recovered in the aqueous phase were used for further quantitative analysis. The protein concentration was determined using the 2-D Quant kit (GE Healthcare, Uppsala, Sweden). Fluorescence labeling of extracted proteins with CyDye DIGE fluors minimal dye (GE Healthcare) was performed according to the manufacturer's instructions and as de-

scribed previously.[37] Supplemental Table S1 at *http://ajp.amjpathol.org* illustrates the study design for the 2-D DIGE experiment. Briefly, protein extracted from normal individuals ($n = 4$) and from PA-treated animals ($n = 4$) were minimally labeled with Cy5 and Cy3 fluorescent dyes (50 μg of protein/400 pmol of dye), respectively, for 30 minutes at 4°C. Additionally, pooled equal aliquots of glomerular extracts from control and PAN animals were labeled with Cy2 fluorescent dye. The reaction was then quenched by the addition of 1 μl of 10 mmol/L lysine. Cy2-, Cy3-, and Cy5-labeled samples were mixed and the volume of the protein mixture was adjusted to 340 μl by adding rehydration buffer containing 7 mol/L urea, 2 mol/L thiourea, and 4% CHAPS. Finally, 15 mmol/L dithiothreitol and 0.5% IPG-buffer were added. Commercial immobilized pH gradient gels (IPG strips, pH 3 to 10 nonlinear, pH 4 to 7, 18 cm; GE Healthcare) were rehydrated with the sample solutions for 12 hours at 20°C and processed as described previously.[36] Each glomerular protein extract was separated twice using IPG strips with a pH range from 3 to 10 nonlinear as well as a pH range from pH 4 to 7 in the first and sodium dodecyl sulfate-polyacrylamide gel electrophoresis (SDS-PAGE) in the second dimension.

Image Acquisition and Visualization of Protein Spots

The Cy2, Cy3, and Cy5 images for each gel were scanned at 488/520-, 532/580-, and 633/670-nm excitation/emission wavelengths, respectively, at 100-μm resolution, thus obtaining a total of 12 images (4×3) using a fluorescence imager (Typhoon 9400, GE Healthcare). PDQuest V7.1 image analysis software (Bio-Rad, Hercules, CA) was used for raw data image analysis of the sample sets including spot detection, matching, and comparison of the protein extracts from control and PAN glomeruli to the pooled standard. Briefly, original images of Cy2, Cy3, and Cy5 images for each gel were cropped, smoothed, and filtered to clarify spots. The Gaussian spots were then created from filtered images and all subsequent spot quantitation and other analyses were done on the Gaussian image. A MatchSet was created for comparing and analyzing spots from all 12 Gaussian images, and a master image, which contains the spot data from all of the gels in the MatchSet, was then generated. The Cy5 and Cy3 spot data from each gel were normalized using respective Cy2 signals of the internal standard. The spot maps of the individual DIGE gels were then used to calculate average abundance changes. The differences were assumed to be significant if the spots were present in all of the gels, with a P value ≤ 0.05 performing the Student's t-test. For subsequent vacuum matrix-assisted laser desorption/ionization mass spectrometry (vMALDI) mass spectrometric analysis the gels were silver-stained according to Blum and colleagues[38] and only protein spots that were visible by silver staining and unambiguously matched to the fluorescence image were picked manually.

Enzymatic Digestion of Proteins and Sample Preparation

In-gel tryptic digestion of selected protein spots and afterward sample purification of ZipTip RP-18 (Millipore, Bedford, MA) purified peptides was performed based on a previously described procedure.[36]

vMALDI Mass Spectrometry—Peptide Mass Fingerprinting (PMF), Postsource Decay (PSD), and High-Energy Collision-Induced Dissociation (CID) Time-of-Flight (TOF)/RTOF

The vMALDI PMF, PSD fragment ion analysis, as well as high-energy CID experiments were performed on a vMALDI time-of-flight (TOF)/curved field reflectron mass spectrometer equipped with a differential pumped high-energy ($E_{Lab} = 20$ keV, collision gas He) CID cell (Axima TOF,[2]; Shimadzu Biotech, Kratos Analytical, Manchester, UK) applying a nitrogen laser (337 nm), as has been previously described.[36] The generated PMF spectra were processed using the company-supplied Savitzky-Golay algorithm and the PSD as well as true high-energy CID spectra were smoothed using the company-supplied algorithm. In all cases the baseline was subtracted. Peak annotation was performed automatically using software provided by the instrument manufacturer (Launchpad, Version 2.7.1.200060929; Shimadzu Biotech, Kratos Analytical).

Database Search for Protein Identification

The peptides of the PMF spectra were manually selected (S/N >2/1 and a plausible isotopic pattern had to be observable), omitting those peptides derived from tryptic autodigestion and matrix-related ions. The generated monoisotopic peptide mass lists were searched using the Mascot search algorithm (*www.matrixscience.com*). Searches were performed using either the SwissProt protein sequence database (version: 46.1, 5148 sequences assigned to *Rattus*) or the NCBI-nonredundant protein sequence database (version: 20050226, 33,598 sequences assigned to *Rattus*) with the following parameters: peptide molecular mass tolerance: ± 0.15 Da; two missed cleavages; cysteine modified by carbamidomethylation; possible modification included oxidation of methionine; taxonomy: *Rattus*. Searches were performed without restriction of protein molecular weight or pI. Raw datasets of the PSD or CID spectra were exported as ASCII files and peaks were manually selected after visual inspection of the spectra. The peptide sequence tags were analyzed by applying two different public available search algorithms, namely Mascot and MS-Tag (ProteinProspector, version 4.0.5, *http://prospector.ucsf.edu*). The search parameters for the PSD and CID data were described previously.[36] The proteins were considered to be positively identified with significant MOWSE scores (P value <0.05) using the PMF data and/or with the unambiguously

identification (P value <0.05) of at least one peptide sequence using the PSD and/or high-energy CID spectra of selected precursor ions (see Supplemental Figures S1 to S23 at *http://ajp.amjpathol.org*).

Cell Culture

Conditionally-immortalized murine podocytes[24] were cultured in RPMI 1640 medium (Gibco BRL) supplemented with 10% fetal calf serum (FCS) and 1% penicillin/streptomycin (Gibco BRL) in the presence of 10 U/ml recombinant mouse interferon-γ (R&D Systems, Minneapolis, MN) at 33°C in 5% CO_2/95% air. To induce differentiation, podocytes were maintained at 37°C in RPMI 1640 supplemented with 10% FCS and 1% penicillin/streptomycin for 10 to 14 days. Cells were seeded in 6-well or 12-well culture dishes for the experiments.

Cell Treatments

For the *in vitro* experiments podocytes were exposed to PA (final concentration, 5 μg/ml; Sigma-Aldrich) for various time periods. In addition, cells were kept unstimulated by adding only carrier to the cells for the same time periods. For some experiments the regular medium was replaced by RPMI 1640 medium containing 1% penicillin/streptomycin and 0.1% FCS supplemented with either 0.1% essentially fatty acid-free BSA (FA-free BSA, 05468, stock solution: 100 mg/ml in phosphate-buffered saline (PBS); Fluka, Buchs, Switzerland) or 0.1% linoleic-oleic-arachidonic acid-albumin from BSA (FA-BSA, stock solution: 100 mg/ml in DPBS, 2 mol each of linoleic acid, oleic acid, and arachidonic acid per mol of albumin, L0163; Sigma-Aldrich).

Sample Preparation and Western Blot Analysis

Preparations of isolated glomeruli from control and PA-treated rats were suspended in 1% Nonidet P-40 buffer (50 mmol/L Tris-buffered saline, 1% Nonidet P-40, and 8 mmol/L ethylenediaminetetraacetic acid) containing protease inhibitors (Complete Protease Inhibitor Cocktail Tablets; Roche Diagnostics, Mannheim, Germany) and were sonicated for 10 minutes at 4°C. Podocyte cell lysates were prepared by homogenization of washed cells in 1% Nonidet P-40 buffer. The glomerular and podocyte cell extracts were purified by centrifugation at 16,000 $\times$ g for 10 minutes and the supernatants were used for further analysis. Proteins solubilized in SDS sample buffer, containing 60 mmol/L Tris, pH 6.8, 10% (v/v) glycerol, 1% SDS, and 100 mmol/L dithiothreitol were used for further analysis. Cell surface proteins of podocytes were labeled and purified by means of the cell surface biotinylation kit (Cell Surface Protein Isolation kit, 89881; Pierce, Rockford, IL) according to the manufacturer's instruction. Briefly, cells cultured in 75-cm^2 flasks were washed in PBS and then incubated with freshly prepared Sulfo-NHS-SS-Biotin (0.25 mg/ml, 2.5 mg per flask) for 30 minutes at 4°C on a rocking platform. The biotinylation reaction was terminated by adding 500 μl of quenching solution and the cells were harvested and washed with Tris-buffered saline (0.025 mol/L Tris, 0.15 mol/L NaCl, pH 7.2). The cell pellet was resuspended in lysis buffer containing protease inhibitors, sonicated, incubated on ice for 30 minutes, and centrifuged for 10,000 $\times$ g for 2 minutes at 4°C. The supernatant containing the solubilized and labeled proteins was further incubated with immobilized NeutrAvidin gel for 1 hour at room temperature with end-over-end mixing. Unbound proteins were removed by four washes with the wash buffer containing protease inhibitors. Biotinylated proteins were then released by incubating with SDS sample buffer, containing 62.5 mmol/L Tris-HCl, pH 6.8, 10% (v/v) glycerol, 1% SDS, and 50 mmol/L dithiothreitol, for 5 minutes at 95°C and subsequent centrifugation. Proteins were resolved by SDS-PAGE using 10% vertical gels and then transferred onto nitrocellulose membranes (Schleicher & Schuell, Dassel, Germany). After blocking with 20% FCS in Tris-buffered saline-T (50 mmol/L Tris, pH 7.6, 150 mmol/L NaCl, 0.02% Tween-20) the membranes were incubated with the respective primary antibodies overnight at 4°C, if not mentioned otherwise, followed by incubation with the appropriate horseradish peroxidase-conjugated secondary antibody, diluted 1:2500 and incubated for 1 hour at room temperature. Detection was performed using an enhanced chemiluminescence assay (GE Healthcare) on a LumiImager work station (Roche). For internal normalization the membranes were reused to detect the expression of glyceraldehyde-3-phosphate dehydrogenase (GAPDH, incubated 1 hour at room temperature). All blots were quantified using the LumiImager software package v3.0 (Roche) and the presented values indicate protein expression levels relative to controls normalized to GAPDH. Statistical analyses were performed using two-tailed Student's unpaired t-test. Significance was rejected at P values ≤ 0.05 and P values ≤ 0.01 were separately noted.

Immunofluorescence Analysis

Cells were fixed in 4% paraformaldehyde for 10 minutes and permeabilized with 0.1% Triton X-100 in PBS for 5 minutes at room temperature. Nonspecific binding sites were saturated by 1% FCS/PBS for 30 minutes at room temperature. Paraformaldehyde-fixed, permeabilized, and blocked cells as well as 2-μm-thick paraffin-embedded kidney sections from control animals ($n = 6$) and PAN rats ($n = 6$) were then incubated with the primary antibody for 1 hour at room temperature. After washing, the primary antibody was detected with the appropriate secondary antibody (Alexa Fluor 488 goat anti-rabbit IgG, Alexa Fluor 488 goat anti-mouse IgG; Molecular Probes, Eugene, OR). As control whole rabbit IgG or whole mouse IgG (Accurate Chemical and Scientific, Westbury, NY) was used instead of the primary antibody and the cells or tissue sections were also incubated with the secondary antibody alone. After immunostaining, the

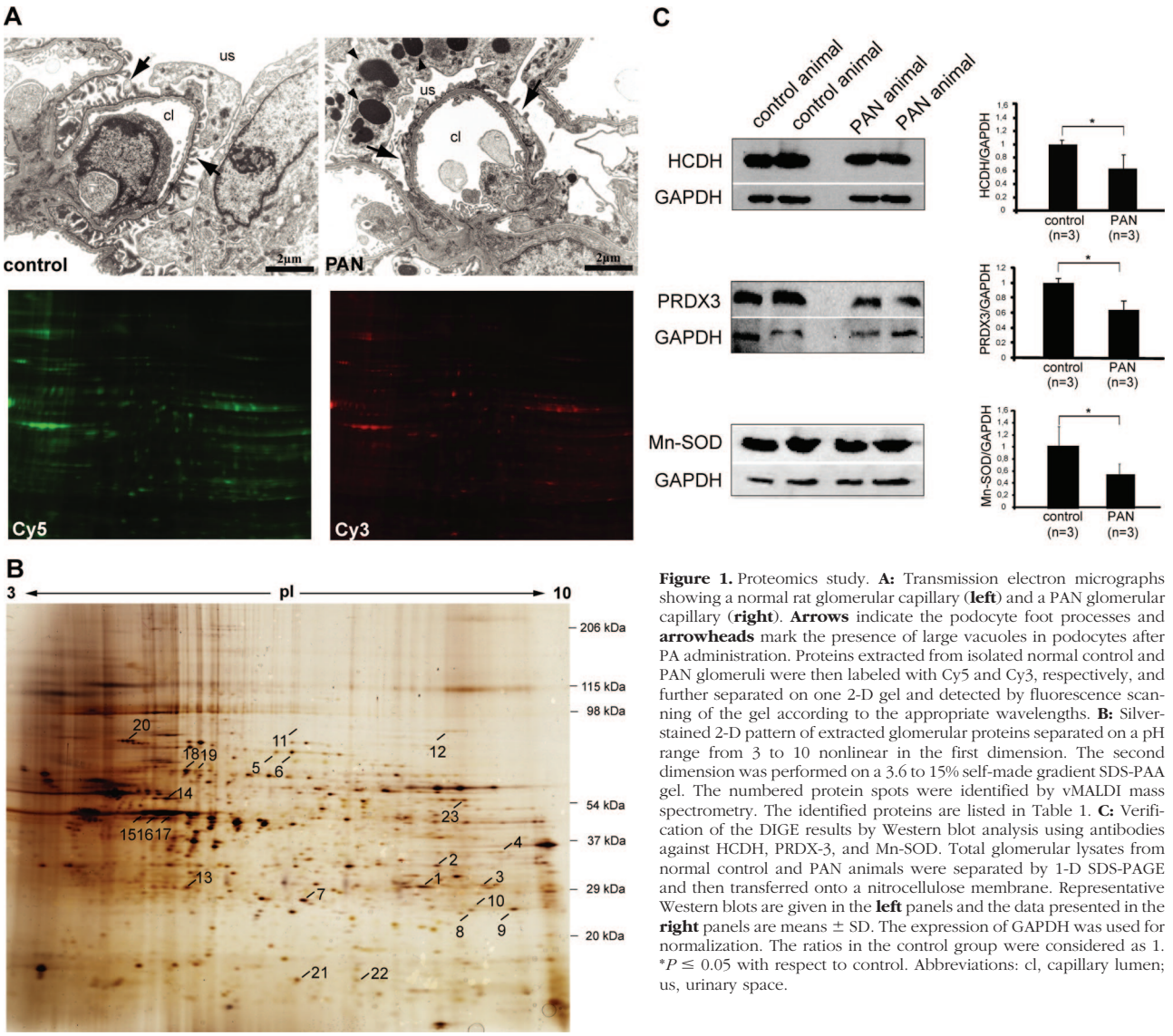

Figure 1. Proteomics study. **A:** Transmission electron micrographs showing a normal rat glomerular capillary (**left**) and a PAN glomerular capillary (**right**). **Arrows** indicate the podocyte foot processes and **arrowheads** mark the presence of large vacuoles in podocytes after PA administration. Proteins extracted from isolated normal control and PAN glomeruli were then labeled with Cy5 and Cy3, respectively, and further separated on one 2-D gel and detected by fluorescence scanning of the gel according to the appropriate wavelengths. **B:** Silver-stained 2-D pattern of extracted glomerular proteins separated on a pH range from 3 to 10 nonlinear in the first dimension. The second dimension was performed on a 3.6 to 15% self-made gradient SDS-PAA gel. The numbered protein spots were identified by vMALDI mass spectrometry. The identified proteins are listed in Table 1. **C:** Verification of the DIGE results by Western blot analysis using antibodies against HCDH, PRDX-3, and Mn-SOD. Total glomerular lysates from normal control and PAN animals were separated by 1-D SDS-PAGE and then transferred onto a nitrocellulose membrane. Representative Western blots are given in the **left** panels and the data presented in the **right** panels are means ± SD. The expression of GAPDH was used for normalization. The ratios in the control group were considered as 1. $^*P \leq 0.05$ with respect to control. Abbreviations: cl, capillary lumen; us, urinary space.

cells were incubated with 4′,6-diamidino-2-phenylindole (DAPI).

Quantitative Real-Time Polymerase Chain Reaction (PCR)

Rat glomeruli from PA-treated as well as control rats (n = 2) were isolated and total RNA was subsequently prepared with AllPrep RNA/protein kit (Qiagen, Duesseldorf, Germany). TaqMan gene expression assays for rCD36 (assay ID: Rn00580728_m1) and rGAPDH (assay ID: Rn99999916_s1) were obtained from Applied Biosystems (Foster City, CA). Random primer-based reverse transcription of mRNA to cDNA was done using the SuperScript kit from Invitrogen (Carlsbad, CA) according to the manufacturer's instructions. Real time PCR was performed on a Chromo4 instrument (Bio-Rad) using TaqMan gene expression master mix (Applied Biosystems) and the relative expression level of rCD36 mRNA was normalized to the amount of rGAPDH in the same sample.

Results

PAN Is Associated with Perturbation in Fatty Acid Metabolism and a Disturbed Antioxidant Defense Mechanism

Electron microscopic examination revealed ultrastructural alterations of the glomerular capillary wall after PA administration as has been described previously[39] and illustrated in Figure 1A. To reduce the sample complexity, glomerular proteins were subjected to Triton X-114 phase separation and proteins recovered in the aqueous phase from isolated normal control glomeruli were then compared with that from PAN glomeruli using 2-D DIGE. This technique includes the differential labeling of samples with fluorescent dyes that can be co-separated on one single 2-D gel. An example is shown in Figure 1A. Hydrophilic proteins from isolated control glomeruli were labeled with Cy5 and an extract from PAN glomeruli was labeled with Cy3. Both samples were separated on a

single 2-D gel and the images were obtained by fluorescence scanning of the gel according to the appropriate wavelengths. In addition an internal standard labeled with Cy2 that consists of a pool of the samples was integrated. This quantitative proteomic approach revealed differential expression (P value ≤ 0.05) of 23 protein spots between these two groups that were unambiguously identified by vMALDI-MS/MS analysis and subsequent database searches (Table 1 and Figure 1B). Supplemental Figures S1 to S23 at *http://ajp.amjpathol.org* show the data of the MS and MS/MS analysis of each of these 23 protein spots.

The vast majority of the proteins were identified with significant score values using the PMF spectra and with at least one peptide, which was fragmented using high-energy CID and/or PSD (Table 1). For some proteins different pI isoforms were picked up (eg, spots 5 and 6). The expressions of 12 proteins were decreased, with expression ratios of 0.79 to 0.31, and 4 were increased with expression ratios of 1.58 to 8.82 in PAN to normal

Table 1. Identification of Differential Expressed Hydrophilic Glomerular Proteins by Means of vMALDI Mass Spectrometry

				PMF		PSD and/or HE CID		
ID	Expr. ratio*	Accession no.†	Protein name	Score‡	%	Precursorion [MH]$^{+}$§	Identified peptide sequence¶	Score
Fatty acid metabolism								
1	0.67	P14604	Enoyl-CoA hydratase, mitochondrial precursor	135	36	2111.08	AQFGQPEILLGTIPGAGGTQR	90
2	0.61	P1380	Electron transfer flavoprotein subunit α, mitochondrial precursor	96	27	1812.84	LLYDLADQLHAAVGASR	58
3	0.35	Q68FU3	Electron-transfer-flavoprotein subunit β, mitochondrial precursor	66	21	2156.05 1339.61	GIHVEVPGAEAENLGPLQVAR VSVISEEPPQR	90, 49
4	0.58	Q9WVK7	Hydroxyacyl-coenzyme A dehydrogenase, mitochondrial precursor	56	20			
5/6	8.82, 7.78	P02770	Serum albumin precursor	97/77	17/13	1465.66 1465.68	LGEYGFQNAVLVR	34, 29
Oxidative stress and detoxification								
7	0.72	Q9Z0V6	Peroxiredoxin-3, mitochondrial precursor	100	28	1206.72 1476.90	HLSVNDLPVGR DYGVLLESAGIALR	68, 65
8/9	0.75/0.79	P07895	Superoxide dismutase (Mn), mitochondrial precursor	102/86	24/28	1004.64 1028.70	NVRPDYLK GELLEAIKR	26/26, 44
10	0.76¶	P04906	Glutathione *S*-transferase P	76	40	1351.80	PPYTIVYFPVR	57
Cytoskeleton								
11	0.39	P31977	Ezrin/moesin	94	24	1182.62	APDFVFYAPR	30
12	5.39	O35763	Ezrin/moesin	41	6	1182.70	APDFVFYAPR	47
13	0.56	Q9EPT8	Chloride intracellular channel 5	95	33	1574.74	HRESNTAGIDIFSK	16
14	1.67	Q4V7C7	Actin-related protein 3 homolog	64	16	1768.85	DREVGIPPEQSLETAK	
15/16/17	0.36/0.37/0.31	P60711 P63259	Actin, cytoplasmic 1/cytoplasmic 2	236/ 223/108	42/41/ 32	1198.66 1791.04 1954.20	AVFPSIVGRPR SYELPDGQVITIGNER VAPEEHPVLLTEAPLNPK	32/55/66 44/69/73 76/59/−
Protein folding								
18/19	0.62/0.79	P63039	Heat shock protein 60 kDa, mitochondrial precursor	57/66	25/28			
20	0.79	P06761	78-kDa glucose-regulated protein precursor	278	40	1566.89 1588.97	ITPSYVAFTPEGRKSDIDEIV LVGGSTR	43, 51
Others								
21/22	6.78/2.88	P02767	Transthyretin precursor	104/113	62/45	1556.71 2517.10	FTEGVYRVELDTK ALGISPFHEYAEVVFTANDSGHR	33/30 74
23	1.58	Q64565	Alanine-glyoxylate aminotransferase 2	88	16	1433.73	LRDEFDIVGDVR	

*Based on PAN/control, derived from the normalized spot volume standardized against the intra-gel standard provided by PDQuest software analysis ($n = 4$, $P \leq 0.05$).

†Accession number from Swiss Prot database.

‡MASCOT probability-based MOWSE (molecular weight search) score calculated for PMF and PSD/HE CID results: score $= -10 \times \log_{10} P$ where P is the absolute probability that the given hit is a random event. Significance ($P < 0.05$) is reached at scores >54 (PMF) and >25 (PSD or HE CID) when searching the NCBI protein database.

§m/z derived from vMALDI PMF analysis.

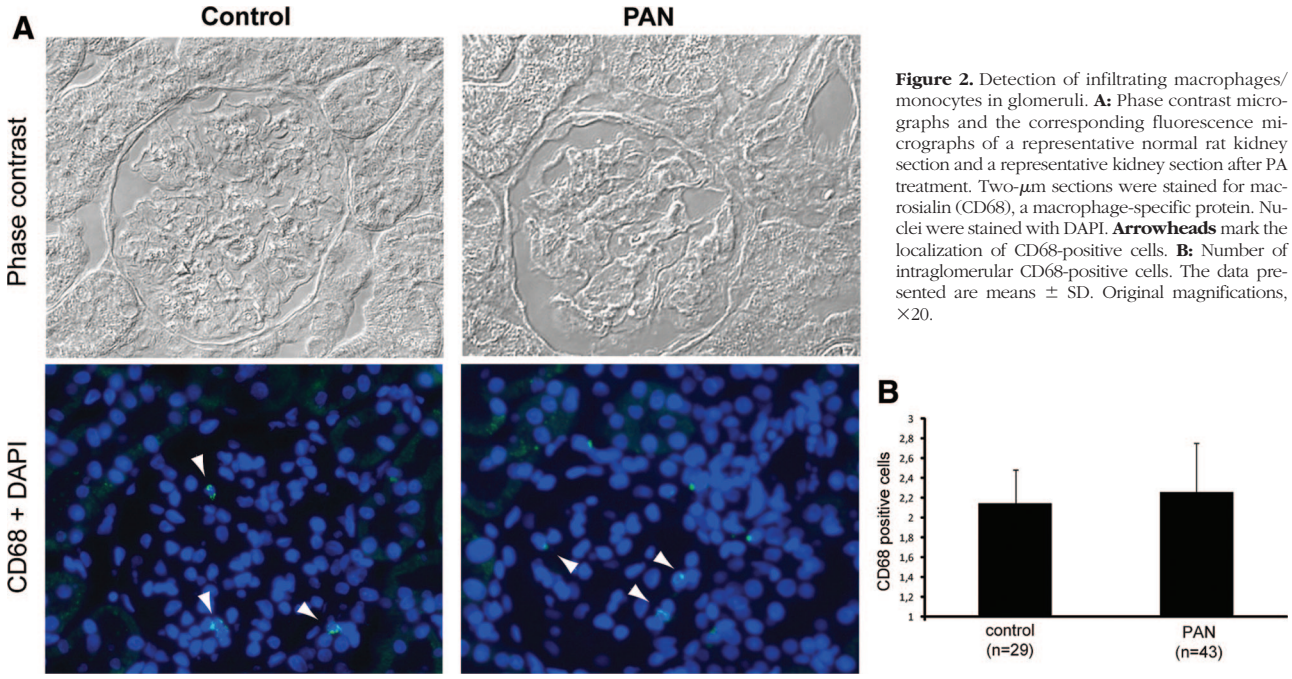

Figure 2. Detection of infiltrating macrophages/monocytes in glomeruli. **A:** Phase contrast micrographs and the corresponding fluorescence micrographs of a representative normal rat kidney section and a representative kidney section after PA treatment. Two-μm sections were stained for macrosialin (CD68), a macrophage-specific protein. Nuclei were stained with DAPI. **Arrowheads** mark the localization of CD68-positive cells. **B:** Number of intraglomerular CD68-positive cells. The data presented are means ± SD. Original magnifications, ×20.

control. The proteins were assigned into groups on the basis of their major cellular functions (based on SwissProt database annotation). Significant differences in protein expression were found related to fatty acid metabolism. Quantitative expression analysis of glomerular proteins defined down-regulation of four key enzymes of the mitochondrial β-oxidation pathway. This group of proteins includes enoyl-CoA hydratase, short chain 3-hydroxylacyl-CoA dehydrogenase (HCDH), electron-transfer flavoprotein α-subunit, and electron-transfer flavoprotein, β-polypeptide. These changes were paralleled with elevated abundance of serum albumin in PAN glomeruli (Table 1). Three key enzymes, ie, peroxiredoxin-3 (PRDX3), Mn-superoxide dismutase (Mn-SOD), and glutathione *S*-transferase P that participates in cellular redox balance were consistently decreased in PAN. Expression of four proteins that play a role in the assembly or maintenance of F-actin-based structures was altered. The same peptide from ezrin/moesin was identified from two different spots, one of them was up-regulated and the other down-regulated. Concomitant with podocyte injury expression of two chaperones were decreased as well. Other proteins affected in PAN were transthyretin, a secreted protein and alanine-glyoxylate aminotransferase 2 precursor, a protein involved in the glyoxylate metabolism. Western blot analyses using appropriate antibodies against selected proteins, namely PRDX3, HCDH, and Mn-SOD, confirmed without exception the MS- and DIGE-based data obtained by the applied proteomic approach by a biological test (Figure 1C). These changes in the glomerular proteome occurred in the absence of a significant difference in the numbers of intraglomerular macrophages in the early PAN rats compared with the control animals (Figure 2).

PA Increases CD36 Expression

The proteomic study points out that PA modulates the expression of enzymes involved in fatty acid metabolism of glomeruli. Therefore we further explored the expression of CD36 that plays a crucial role in the uptake and transport of fatty acids.[40,41] Using a polyclonal antibody against CD36, two different variants with molecular weights of 88 kDa and 53 kDa, corresponding to the glycosylated and the nonglycosylated form, respectively,[42–44] were detected by Western blot (Figure 3A). Quantitative Western blot analysis revealed that both vari-

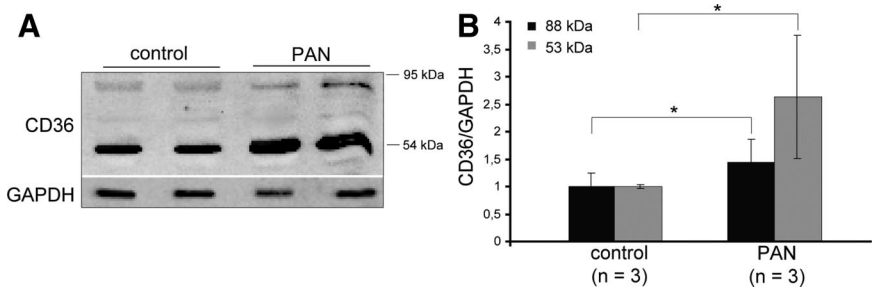

Figure 3. Effect of PA on CD36. Western blot analysis of CD36 expression using glomerular lysates from control normal as well as PA-treated animals. A representative Western blot is given in **A** and the data presented in **B** are means (n = 3 in each group) ± SD. The expression of GAPDH was used for normalization. The ratios in the control group were considered as 1. $^*P \leq 0.05$ with respect to control.

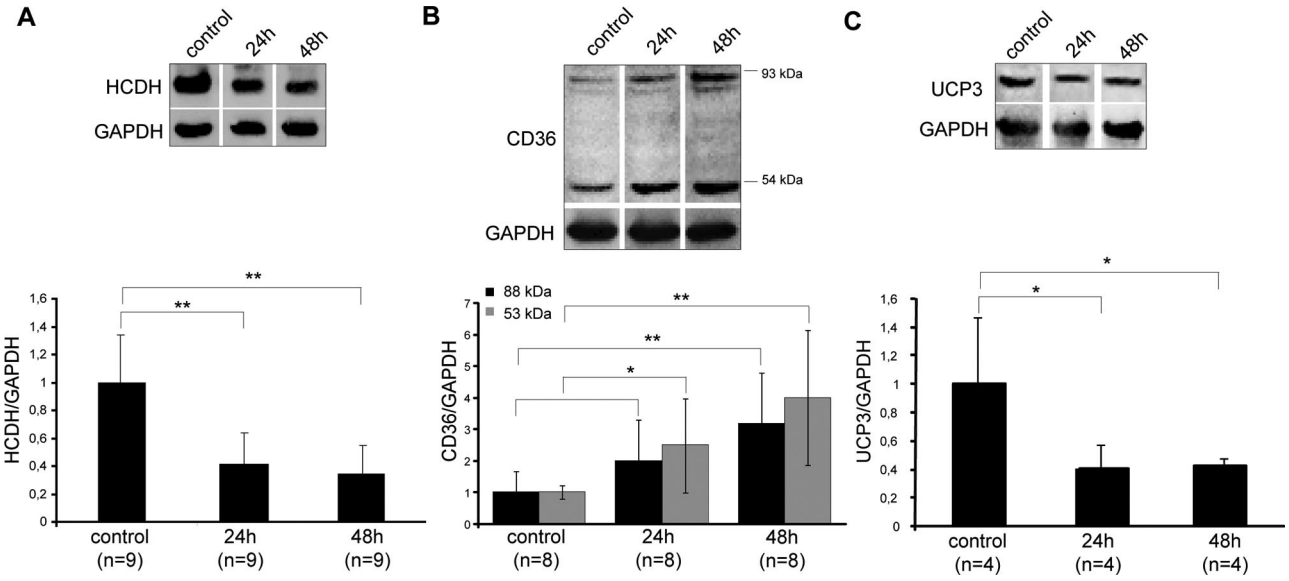

Figure 4. Effect of PA on proteins involved in fatty acid metabolism in podocytes *in vitro*. Cultivated podocytes were either untreated or treated with 5 μg/ml of PA for 24 or 48 hours and the protein expression of HCDH (**A**), CD36 (**B**), and UCP3 (**C**) was examined by Western blotting. In each case a representative Western blot is given in the **top** panel and the data presented in the **bottom** panel are means ± SD. The expression of GAPDH was used for normalization. The ratios in the control group were considered as 1. $^{*}P \leq 0.05$ and $^{**}P \leq 0.01$ with respect to control.

ants of CD36 were significantly ($P \leq 0.05$) increased in early stages of PAN. The 88-kDa form was increased 1.43-fold and the lower molecular weight variant was increased 2.63-fold (Figure 3B). Quantitative real-time PCR indicated also an increased CD36 mRNA level in PAN glomeruli (213.4 ± 104.7) compared with control glomeruli (100.0 ± 29.9).

PA Modulates the Expression of Proteins Involved in Fatty Acid Metabolism in Podocytes in Vitro

To confirm that these changes were related to podocytes, and not to other glomerular cell types, we next analyzed the expression of proteins that handle fatty acids *in vitro* using conditionally immortalized mouse podocytes that were exposed to 5 μg/ml of PA for different time periods. As shown in Figure 4A, HCDH was already reduced 2.4-fold after 24 hours and further decreased after 48 hours of PA treatment.

CD36 protein expression was induced in response to PA treatment (Figure 4B). The glycosylated form was increased 2-fold after 24 hours and increased further to 3.2-fold ($P \leq 0.01$) after 48 hours, when compared with untreated cells. The protein level of the nonglycosylated form was increased already up to fourfold ($P \leq 0.01$) after 48 hours exposure to PA. Furthermore, the protein expression of mitochondrial uncoupling protein 3 (UCP3), a member of the mitochondrial carrier family,[45,46] was reduced in response to PA treatment. Already after 24 hours the UCP3 content decreased 2.5-fold and remained lowered after 48 hours of incubation with PA compared with control untreated cells (Figure 4C).

CD36 Is Expressed on the Cell Surface of Podocytes in Vitro

Subsequently we studied the cellular localization of CD36. Immunofluorescence staining exhibited that CD36 was predominantly localized to the plasma membrane (Figure 5A). In addition staining of various intracellular, vesicular structures throughout the cell was seen. The surface localization of CD36 in podocytes was further assessed by cell surface biotinylation and neutravidin precipitation. As illustrated in Figure 5B, Western blot analysis shows that the glycosylated form of CD36 was highly enriched in the precipitate, revealing surface localization of the protein. To determine the purity of the isolated cell surface fraction Western blots using antibodies against Mn-SOD and against α-dystroglycan (α-DG) were performed as well. Whereas Mn-SOD, a protein that is localized to mitochondria,[47] was not detectable in the precipitated protein fraction and only found in the total cell lysate, α-DG, a plasma membrane protein,[48] was highly enriched at the cell surface (Figure 5B).

Albumin-Bound Fatty Acids Affect Mn-SOD Expression

Next we explored expression of Mn-SOD that is a major mitochondrial antioxidant in cultured podocytes. Under normal culturing conditions the protein content significantly increased 1.35-fold after 24 hours of PA treatment, but longer incubation resulted in a 1.55-fold down-regulation of Mn-SOD (Figure 6A). Furthermore we investigated the effect of albumin and albumin-bound fatty acids on protein expression. After exposure to PA for 24

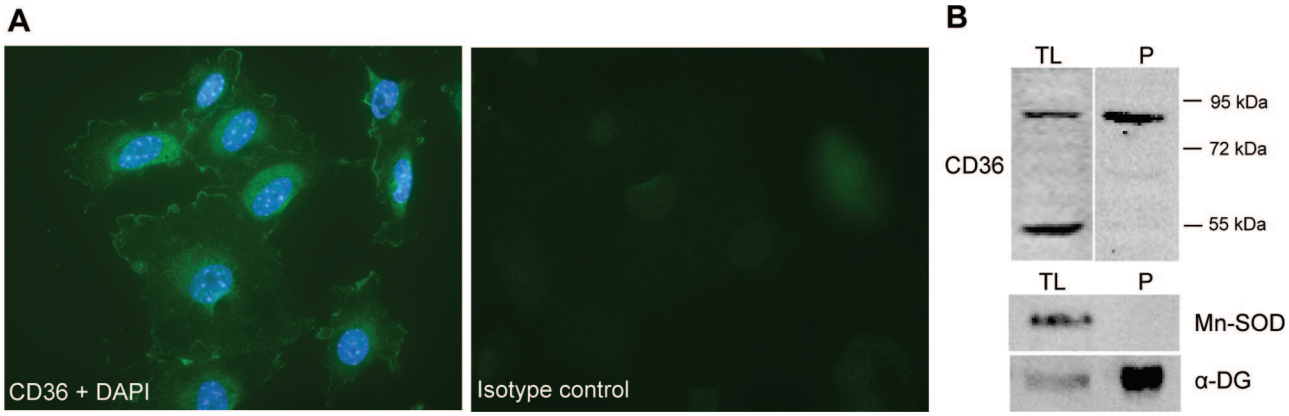

Figure 5. Subcellular localization of CD36. **A:** Fluorescence micrograph of cultured podocytes that were exposed to PA for 24 hours. Cells were fixed, permeabilized, and stained with CD36 (diluted 1:200 and incubated for 1 hour at room temperature) using an Alexa Fluor 488-conjugated secondary antibody (diluted 1:1000 and incubated for 1 hour at room temperature). Nuclei were stained with DAPI. To verify the specificity of the antibody, cells were incubated with unspecific rabbit IgG. **B:** Podocytes that were exposed to PA for 24 hours were biotin-labeled on the cell surface and protein extracts (TL) without and after purification (P) with NeutrAvidin gel were separated by 1-D SDS-PAGE and transferred onto nitrocellulose. Western blotting was performed using antibodies against CD36, Mn-SOD, and α-DG. The positions of molecular mass markers are indicated at the right. Original magnifications, ×40.

hours an induction of the protein level could be seen in cells cultured with 0.1% FCS alone or supplemented with either 0.1% FA-free BSA or 0.1% FA-BSA (data not shown). But, after prolonged exposure of the cells to PA, expression of Mn-SOD decreased in the presence of albumin-bound fatty acids, whereas in the absence the protein content remained elevated (Figure 6B).

Discussion

Podocytes play an important role in the maintenance of the glomerular filtration barrier. Understanding of the molecular mechanisms leading to injury is therefore necessary to prevent or to reduce loss of filtration function. To elucidate cellular changes in association with podocyte damage and glomerular dysfunction the investigation of a well-established experimental renal disease provides an excellent opportunity. The course of PAN and the alterations that occur in the glomerular capillary wall in response to daily injection of PA have been described by a number of investigators.[39,49] In this study animals treated for 5 days were examined because they represent an early stage in the disease at which time the glomerular changes are minimal and restricted to the podocytes.[13,49]

To get a deeper insight into the cellular processes occurring at this specific time point we used a proteomic-based approach to characterize protein expression changes in glomeruli. The presented data clearly indicated that different functional groups of proteins are linked to impairment of the filtration barrier induced by PA. The key finding was that proteins involved in the transport and oxidation of fatty acids were intimately connected with early stages of PAN *in vivo*. Four enzymes of the complex mitochondrial β-oxidation pathway were down-regulated, suggesting defective degradation of fatty acids. Albumin and CD36 were elevated in protein extracts from PAN glomeruli. Divergent expression of fatty acid-using proteins could be shown in cultured podocytes exposed to PA *in vitro* as well. Moreover, we demonstrated not only the coordinated down-regulation of enzymes of the cellular antioxidant defense mechanisms in PAN *in vivo* but the modulatory effects of albumin-bound fatty acids on the expression of Mn-SOD in PA-induced podocyte lesions. These findings provide a novel illumination of some cellular events leading to podocyte dysfunction.

Fatty acids are ubiquitous substrates for a variety of cellular processes including protein modification, membrane biosynthesis, or generation of lipid-containing messengers in signal transduction and are substrates for mitochondrial energy conversion.[50,51] On activation to their respective coenzyme A (CoA) esters in cytoplasm, fatty acids are degraded to acetyl-CoA in the mitochondrial matrix by β-oxidation, which functions either to directly produce ATP or to produce ketone bodies for ATP

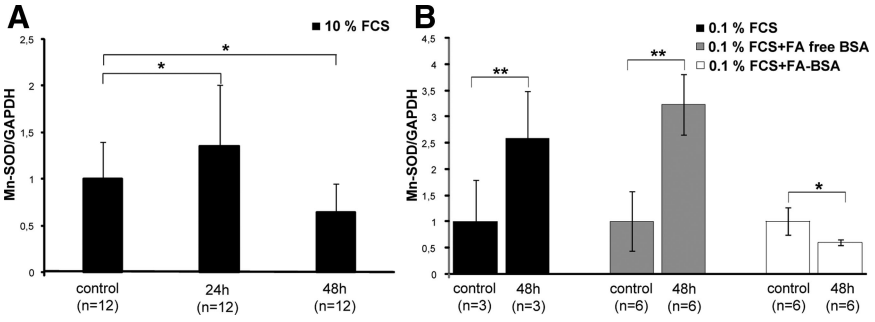

Figure 6. PA induced-changes in the protein expression of Mn-SOD. **A:** Podocytes were either untreated or treated with PA for 24 and 48 hours in regular culture medium containing 10% FCS and the protein expression of Mn-SOD was examined by Western blotting. **B:** Podocytes cultured in medium containing 0.1% FCS either alone or supplemented with 0.1% fatty acid (FA)-free BSA or 0.1% FA bound to albumin exposed to PA for 48 hours. The values are the means ± SD. The expression of GAPDH was used for normalization. The ratio in the control group was considered as 1. $^{*}P \leq 0.05$ and $^{**}P \leq 0.01$ with respect to control.

generation.[52] Disturbances in fatty acid metabolism and regulation, especially involving fatty acid synthesis and oxidation, can contribute to hyperlipidemia, obesity, and insulin resistance.[50] The uptake of fatty acids from the circulation into cells consists of several steps the sequence including the fatty acid dissociation from albumin followed by binding to plasma membrane proteins or integration into the lipid bilayer and their transport across the plasma membranes.[53]

Various studies have shown that CD36 that is a multifunctional protein is a key molecule in the uptake of long-chain fatty acids.[54,55] So far CD36 was found on several cell types, including platelets and macrophages,[41,56] and has also been localized to human and rat skeletal mitochondria.[55,57] In this study we show by immunofluorescence microscopy and Western blot analysis of cell surface biotinylated proteins that CD36 is expressed on the cell surface of podocytes *in vitro*.

Changes in CD36 expression and subcellular distribution have been linked to FA uptake.[40,58,59] Palanivel and colleagues[60] described that enhanced fatty acid uptake mediated by increased CD36 expression together with a depressed β-oxidation led to intracellular lipid accumulation. Accumulated fatty acids that are trapped into the mitochondrial matrix, which is the major site of mitochondrial ROS production, are targets for lipid peroxidation via ROS and presumably result in LPO-induced mitochondrial damage and dysfunction.[61,62]

Thus, the PA-induced disturbances of fatty acid metabolism including the up-regulation of CD36 linked to decreased enzymes level of fatty acid degradation, may be a critical cause of enhanced LPO. These are essential findings as the importance of LPO in the production of proteinuria in PAN has been demonstrated by a number of studies.[25,63,64] In addition, UCP3, a member of the family of mitochondrial inner membrane anion carrier proteins[65] was decreased in podocytes exposed to PA. The protein has been suggested to be involved in the transport of fatty acid anions from the mitochondrial matrix.[45,46] Schrauwen and colleagues[45] postulated that UCP3 is in this way involved in the protection of mitochondria against accumulation of nonesterified fatty acids in the mitochondrial matrix and LPO. A previous study showed also a direct association between elevated oxidative stress and Ucp3$^{-/-}$ mitochondria.[66] Thus, a decreased expression on exposure to PA in association with an increased CD36 level might additionally account for LPO and oxidative stress in podocytes.

Accordingly the coordinated down-regulation of key enzymes of the cellular antioxidant defense may contribute in part to oxidative stress, which occurs whenever an imbalance between ROS production and detoxification exists.[67] Several studies provided evidence that ROS play a pivotal role in PAN.[18,20,68,69] Furthermore, Beaman and colleagues[70] suggested that superoxide anion and hydrogen peroxide or their reaction products are involved in glomerular injury. In the present study we demonstrate that Mn-SOD that catalyzes the dismutation of superoxide radical into oxygen and hydrogen peroxide[71] and PRDX3 a mitochondrial protein that reduces hydrogen peroxide[72] are decreased at the early stages of PAN strongly supporting this observation.

We provide further evidence that the disturbed fatty acid utilization is linked to the impaired antioxidant response in podocytes exposed to PA. The presence of fatty acids bound to albumin led to down-regulation of Mn-SOD after sustained exposure to PA in podocytes, closely resembling the *in vivo* situation. This may be a result of increased fatty acid uptake in response to PA because of enhanced CD36 protein expression. According to our *in vivo* and *in vitro* findings PA might be directly responsible for increased expression of CD36 on the protein but also on the mRNA level. We also observed the immensely enriched abundance of serum albumin precursor that serves as main transporter of fatty acids in the plasma[73] in isolated PAN glomeruli and Ghiggeri and colleagues[74] demonstrated that in MCD the urinary albumin is defatted.

In conclusion, the proteomics strategy was an effective approach to profile glomerular proteins and offered new insights into the molecular mechanism of PAN. The presented data provide evidence that a disturbed transport and oxidation of fatty acids paralleled by an impaired antioxidant response contribute to the pathogenesis of early stages of PA-induced podocyte and glomerular lesions, possibly attributable to fatty acid accumulation and lipid peroxidation in association with deficient antioxidative response. These changes were observed in isolated glomeruli *in vivo*, and also in cultured podocytes *in vitro*, corresponding to the central role of these cells in the maintenance of glomerular filtration function.

Acknowledgment

We thank Ingrid Raab for expert technical assistance.

References

1. Miner JH: A molecular look at the glomerular barrier. Nephron Exp Nephrol 2003, 94:e119–e122
2. Brenner BM, Hostetter TH, Humes HD: Glomerular permselectivity: barrier function based on discrimination of molecular size and charge. Am J Physiol 1978, 234:F455–F460
3. Bohrer MP, Deen WM, Robertson CR, Troy JL, Brenner BM: Influence of molecular configuration on the passage of macromolecules across the glomerular capillary wall. J Gen Physiol 1979, 74:583–593
4. Chang RL, Deen WM, Robertson CR, Brenner BM: Permselectivity of the glomerular capillary wall: III. Restricted transport of polyanions. Kidney Int 1975, 8:212–218
5. Kanwar YS, Liu ZZ, Kashihara N, Wallner EI: Current status of the structural and functional basis of glomerular filtration and proteinuria. Semin Nephrol 1991, 11:390–413
6. Rennke HG, Olson JL, Venkatachalam MA: Glomerular filtration of macromolecules: normal mechanisms and the pathogenesis of proteinuria. Contrib Nephrol 1981, 24:30–41
7. Kerjaschki D: Dysfunctions of cell biological mechanisms of visceral epithelial cell (podocytes) in glomerular diseases. Kidney Int 1994, 45:300–313
8. Farquhar MG, Vernier RL, Good RA: An electron microscope study of the glomerulus in nephrosis, glomerulonephritis, and lupus erythematosus. J Exp Med 1957, 106:649–660
9. Farquhar MG, Vernier RL, Good RA: Studies on familial nephrosis. II. Glomerular changes observed with the electron microscope. Am J Pathol 1957, 33:791–817

10. Barisoni L, Mundel P: Podocyte biology and the emerging understanding of podocyte diseases. Am J Nephrol 2003, 23:353–360
11. van den Berg JG, Weening JJ: Role of the immune system in the pathogenesis of idiopathic nephrotic syndrome. Clin Sci (Lond) 2004, 107:125–136
12. Ryan GB, Karnovsky MJ: An ultrastructural study of the mechanisms of proteinuria in aminonucleoside nephrosis. Kidney Int 1975, 8:219–232
13. Vernier RL, Papermaster BW, Good RA: Aminonucleoside nephrosis: I. Electron microscopic study of the renal lesion in rats. J Exp Med 1959, 109:115–126
14. Luimula P, Sandstrom N, Novikov D, Holthofer H: Podocyte-associated molecules in puromycin aminonucleoside nephrosis of the rat. Lab Invest 2002, 82:713–718
15. Smoyer WE, Mundel P, Gupta A, Welsh MJ: Podocyte alpha-actinin induction precedes foot process effacement in experimental nephrotic syndrome. Am J Physiol 1997, 273:F150–F157
16. Whiteside CI, Cameron R, Munk S, Levy J: Podocytic cytoskeletal disaggregation and basement-membrane detachment in puromycin aminonucleoside nephrosis. Am J Pathol 1993, 142:1641–1653
17. Zou J, Yaoita E, Watanabe Y, Yoshida Y, Nameta M, Li H, Qu Z, Yamamoto T: Upregulation of nestin, vimentin, and desmin in rat podocytes in response to injury. Virchows Arch 2006, 448:485–492
18. Diamond JR, Bonventre JV, Karnovsky MJ: A role for oxygen free radicals in aminonucleoside nephrosis. Kidney Int 1986, 29:478–483
19. Kojima K, Matsui K, Nagase M: Protection of alpha(3) integrin-mediated podocyte shape by superoxide dismutase in the puromycin aminonucleoside nephrosis rat. Am J Kidney Dis 2000, 35:1175–1185
20. Thakur V, Walker PD, Shah SV: Evidence suggesting a role for hydroxyl radical in puromycin aminonucleoside-induced proteinuria. Kidney Int 1988, 34:494–499
21. Neale TJ, Ojha PP, Exner M, Poczewski H, Ruger B, Witztum JL, Davis P, Kerjaschki D: Proteinuria in passive Heymann nephritis is associated with lipid peroxidation and formation of adducts on type IV collagen. J Clin Invest 1994, 94:1577–1584
22. Holthöfer H, Kretzler M, Haltia A, Solin ML, Taanman JW, Schagger H, Kriz W, Kerjaschki D, Schlondorff D: Altered gene expression and functions of mitochondria in human nephrotic syndrome. FASEB J 1999, 13:523–532
23. Binder CJ, Weiher H, Exner M, Kerjaschki D: Glomerular overproduction of oxygen radicals in Mpv17 gene-inactivated mice causes podocyte foot process flattening and proteinuria: a model of steroid-resistant nephrosis sensitive to radical scavenger therapy. Am J Pathol 1999, 154:1067–1075
24. Mundel P, Reiser J, Zuniga Mejia Borja A, Pavenstadt H, Davidson GR, Kriz W, Zeller R: Rearrangements of the cytoskeleton and cell contacts induce process formation during differentiation of conditionally immortalized mouse podocyte cell lines. Exp Cell Res 1997, 236:248–258
25. Vega-Warner V, Ransom RF, Vincent AM, Brosius FC, Smoyer WE: Induction of antioxidant enzymes in murine podocytes precedes injury by puromycin aminonucleoside. Kidney Int 2004, 66:1881–1889
26. Smoyer WE, Ransom RF: Hsp27 regulates podocyte cytoskeletal changes in an in vitro model of podocyte process retraction. FASEB J 2002, 16:315–326
27. Bi X, Lin Q, Foo TW, Joshi S, You T, Shen HM, Ong CN, Cheah PY, Eu KW, Hew CL: Proteomic analysis of colorectal cancer reveals alterations in metabolic pathways: mechanism of tumorigenesis. Mol Cell Proteomics 2006, 5:1119–1130
28. Tessari P, Puricelli L, Iori E, Arrigoni G, Vedovato M, James P, Coracina A, Millioni R: Altered chaperone and protein turnover regulators expression in cultured skin fibroblasts from type 1 diabetes mellitus with nephropathy. J Proteome Res 2007, 6:976–986
29. Barati MT, Merchant ML, Kain AB, Jevans AW, McLeish KR, Klein JB: Proteomic analysis defines altered cellular redox pathways and advanced glycation end-product metabolism in glomeruli of db/db diabetic mice. Am J Physiol 2007, 293:F1157–F1165
30. Xu BJ, Shyr Y, Liang X, Ma LJ, Donnert EM, Roberts JD, Zhang X, Kon V, Brown NJ, Caprioli RM, Fogo AB: Proteomic patterns and prediction of glomerulosclerosis and its mechanisms. J Am Soc Nephrol 2005, 16:2967–2975
31. Kerjaschki D: Membrane Protein Antigens and Other Molecules on Glomerular Cells. Edited by Neilson EG, Couser WG. Philadelphia, Lippincott-Raven Publisher, 1997, pp 203–216
32. Mayrhofer C, Krieger S, Allmaier G, Kerjaschki D: DIGE compatible labelling of surface proteins on vital cells in vitro and in vivo. Proteomics 2006, 6:579–585
33. Farquhar MG, Palade GE: Glomerular permeability. II. Ferritin transfer across the glomerular capillary wall in nephrotic rats. J Exp Med 1961, 114:699–716
34. Kojima K, Davidovits A, Poczewski H, Langer B, Uchida S, Nagy-Bojarski K, Hovorka A, Sedivy R, Kerjaschki D: Podocyte flattening and disorder of glomerular basement membrane are associated with splitting of dystroglycan-matrix interaction. J Am Soc Nephrol 2004, 15:2079–2089
35. Breiteneder-Geleff S, Matsui K, Soleiman A, Meraner P, Poczewski H, Kalt R, Schaffner G, Kerjaschki D: Podoplanin, novel 43-kd membrane protein of glomerular epithelial cells, is down-regulated in puromycin nephrosis. Am J Pathol 1997, 151:1141–1152
36. Mayrhofer C, Krieger S, Raptakis E, Allmaier G: Comparison of vacuum matrix-assisted laser desorption/ionization (MALDI) and atmospheric pressure MALDI (AP-MALDI) tandem mass spectrometry of 2-dimensional separated and trypsin-digested glomerular proteins for database search derived identification. J Proteome Res 2006, 5:1967–1978
37. Chang MW, Grillari J, Mayrhofer C, Fortschegger K, Allmaier G, Marzban G, Katinger H, Voglauer R: Comparison of early passage, senescent and hTERT immortalized endothelial cells. Exp Cell Res 2005, 309:121–136
38. Blum H, Beier H, Gross HJ: Improved silver staining of plant proteins, RNA and DNA in polyacrylamide gels. Electrophoresis 2005, 8:93–99
39. Harkin JC, Recant L: Pathogenesis of experimental nephrosis electron microscopic observations. Am J Pathol 1960, 36:303–329
40. Febbraio M, Abumrad NA, Hajjar DP, Sharma K, Cheng W, Pearce SF, Silverstein RL: A null mutation in murine CD36 reveals an important role in fatty acid and lipoprotein metabolism. J Biol Chem 1999, 274:19055–19062
41. Febbraio M, Hajjar DP, Silverstein RL: CD36: a class B scavenger receptor involved in angiogenesis, atherosclerosis, inflammation, and lipid metabolism. J Clin Invest 2001, 108:785–791
42. Greenwalt DE, Lipsky RH, Ockenhouse CF, Ikeda H, Tandon NN, Jamieson GA: Membrane glycoprotein CD36: a review of its roles in adherence, signal transduction, and transfusion medicine. Blood 1992, 80:1105–1115
43. Gruarin P, Sitia R, Alessio M: Formation of one or more intrachain disulphide bonds is required for the intracellular processing and transport of CD36. Biochem J 1997, 328:635–642
44. Zeng Y, Tao N, Chung KN, Heuser JE, Lublin DM: Endocytosis of oxidized low density lipoprotein through scavenger receptor CD36 utilizes a lipid raft pathway that does not require caveolin-1. J Biol Chem 2003, 278:45931–45936
45. Schrauwen P, Saris WH, Hesselink MK: An alternative function for human uncoupling protein 3: protection of mitochondria against accumulation of nonesterified fatty acids inside the mitochondrial matrix. FASEB J 2001, 15:2497–2502
46. Himms-Hagen J, Harper ME: Physiological role of UCP3 may be export of fatty acids from mitochondria when fatty acid oxidation predominates: an hypothesis. Exp Biol Med (Maywood) 2001, 226:78–84
47. Zhyvoloup A, Nemazanyy I, Panasyuk G, Valovka T, Fenton T, Rebholz H, Wang ML, Foxon R, Lyzogubov V, Usenko V, Kyyamova R, Gorbenko O, Matsuka G, Filonenko V, Gout IT: Subcellular localization and regulation of coenzyme A synthase. J Biol Chem 2003, 278:50316–50321
48. Kerjaschki D: Caught flat-footed: podocyte damage and the molecular bases of focal glomerulosclerosis. J Clin Invest 2001, 108:1583–1587
49. Caulfield JP, Farquhar MG: The permeability of glomerular capillaries of aminonuceoside nephrotic rats to graded dextrans. J Exp Med 1975, 142:61–83
50. Reddy JK: Nonalcoholic steatosis and steatohepatitis. III. Peroxisomal beta-oxidation, PPAR alpha, and steatohepatitis. Am J Physiol 2001, 281:G1333–G1339
51. van der Vusse GJ, van Bilsen M, Glatz JF, Hasselbaink DM, Luiken JJ: Critical steps in cellular fatty acid uptake and utilization. Mol Cell Biochem 2002, 239:9–15
52. Bartlett K, Eaton S: Mitochondrial beta-oxidation. Eur J Biochem 2004, 271:462–469

53. Doege H, Stahl A: Protein-mediated fatty acid uptake: novel insights from in vivo models. Physiology (Bethesda) 2006, 21:259–268
54. Abumrad NA, el-Maghrabi MR, Amri EZ, Lopez E, Grimaldi PA: Cloning of a rat adipocyte membrane protein implicated in binding or transport of long-chain fatty acids that is induced during preadipocyte differentiation. Homology with human CD36. J Biol Chem 1993, 268:17665–17668
55. Bezaire V, Bruce CR, Heigenhauser GJ, Tandon NN, Glatz JF, Luiken JJ, Bonen A, Spriet LL: Identification of fatty acid translocase on human skeletal muscle mitochondrial membranes: essential role in fatty acid oxidation. Am J Physiol 2006, 290:E509–E515
56. Endemann G, Stanton LW, Madden KS, Bryant CM, White RT, Protter AA: CD36 is a receptor for oxidized low density lipoprotein. J Biol Chem 1993, 268:11811–11816
57. Campbell SE, Tandon NN, Woldegiorgis G, Luiken JJ, Glatz JF, Bonen A: A novel function for fatty acid translocase (FAT)/CD36: involvement in long chain fatty acid transfer into the mitochondria. J Biol Chem 2004, 279:36235–36241
58. Ibrahimi A, Abumrad NA: Role of CD36 in membrane transport of long-chain fatty acids. Curr Opin Clin Nutr Metab Care 2002, 5:139–145
59. Bonen A, Campbell SE, Benton CR, Chabowski A, Coort SL, Han XX, Koonen DP, Glatz JF, Luiken JJ: Regulation of fatty acid transport by fatty acid translocase/CD36. Proc Nutr Soc 2004, 63:245–249
60. Palanivel R, Eguchi M, Shuralyova I, Coe I, Sweeney G: Distinct effects of short- and long-term leptin treatment on glucose and fatty acid uptake and metabolism in HL-1 cardiomyocytes. Metabolism 2006, 55:1067–1075
61. Schrauwen P, Hesselink MK: Oxidative capacity, lipotoxicity, and mitochondrial damage in type 2 diabetes. Diabetes 2004, 53:1412–1417
62. Hoeks J, Hesselink MK, Sluiter W, Schaart G, Willems J, Morrisson A, Clapham JC, Saris WH, Schrauwen P: The effect of high-fat feeding on intramuscular lipid and lipid peroxidation levels in UCP3-ablated mice. FEBS Lett 2006, 580:1371–1375
63. Cheng ZZ, Patari A, Aalto-Setala K, Novikov D, Schlondorff D, Holthofer H: Hypercholesterolemia is a prerequisite for puromycin inducible damage in mouse kidney. Kidney Int 2003, 63:107–112
64. Fawcett JP, Jiang R, Walker RJ: Time course of lipid peroxidation in puromycin aminonucleoside-induced nephropathy. Res Commun Mol Pathol Pharmacol 1994, 86:227–234
65. Seifert EL, Bezaire V, Estey C, Harper ME: Essential role for uncoupling protein-3 in mitochondrial adaptation to fasting but not in fatty acid oxidation or fatty acid anion export. J Biol Chem 2008, 283:25124–25131
66. Brand MD, Pamplona R, Portero-Otin M, Requena JR, Roebuck SJ, Buckingham JA, Clapham JC, Cadenas S: Oxidative damage and phospholipid fatty acyl composition in skeletal muscle mitochondria from mice underexpressing or overexpressing uncoupling protein 3. Biochem J 2002, 368:597–603
67. Cemek M, Caksen H, Bayiroglu F, Cemek F, Dede S: Oxidative stress and enzymic-non-enzymic antioxidant responses in children with acute pneumonia. Cell Biochem Funct 2006, 24:269–273
68. Ricardo SD, Bertram JF, Ryan GB: Reactive oxygen species in puromycin aminonucleoside nephrosis: in vitro studies. Kidney Int 1994, 45:1057–1069
69. Gwinner W, Landmesser U, Brandes RP, Kubat B, Plasger J, Eberhard O, Koch KM, Olbricht CJ: Reactive oxygen species and antioxidant defense in puromycin aminonucleoside glomerulopathy. J Am Soc Nephrol 1997, 8:1722–1731
70. Beaman M, Birtwistle R, Howie AJ, Michael J, Adu D: The role of superoxide anion and hydrogen peroxide in glomerular injury induced by puromycin aminonucleoside in rats. Clin Sci (Lond) 1987, 73:329–332
71. Fridovich I: Superoxide radical and superoxide dismutases. Annu Rev Biochem 1995, 64:97–112
72. Cao Z, Bhella D, Lindsay JG: Reconstitution of the mitochondrial PrxIII antioxidant defence pathway: general properties and factors affecting PrxIII activity and oligomeric state. J Mol Biol 2007, 372:1022–1033
73. Stremmel W, Pohl L, Ring A, Herrmann T: A new concept of cellular uptake and intracellular trafficking of long-chain fatty acids. Lipids 2001, 36:981–989
74. Ghiggeri GM, Ginevri F, Candiano G, Oleggini R, Perfumo F, Queirolo C, Gusmano R: Characterization of cationic albumin in minimal change nephropathy. Kidney Int 1987, 32:547–553